Haemodynamic changes in the fetal circulation post-connection to an artificial placenta: a computational modelling study

M. Inmaculada Villanueva[1], Marc López[2], Sergio Sánchez[3], Patricia Garcia-Cañadilla[3,4], Paula C. Randanne[3], Ameth Hawkins[3], Elisenda Eixarch[3], Elisenda Bonet[3], Eduard Gratacós[3], Fàtima Crispi[2,3], Bart Bijnens[3,5], and Gabriel Bernardino[6]

[1] Physense, DTIC, Universitat Pompeu Fabra, Barcelona, Spain
[2] Universitat de Barcelona, Barcelona, Spain
[3] BCNatal - Barcelona Center for Maternal-Fetal and Neonatal Medicine (Hospital Sant Joan de Déu and Hospital Clínic, August Pi i Sunyer Biomedical Research Institute (IDIBAPS), University of Barcelona), Barcelona, Spain
[4] Cardiovascular Diseases and Child Development,Institut de Recerca Sant Joan de Déu, Esplugues de Llobregat, Spain
[5] ICREA - Catalan Institution for Research and Advanced Studies, Barcelona, Spain
[6] Univ Lyon, Université Claude Bernard Lyon 1, INSA-Lyon, CNRS, Inserm, CREATIS UMR 5220, U1294, F-69621, Lyon, France

Abstract. Artificial placenta (AP) is a promising approach to improve survival in extremely premature fetuses, removing them from the uterus and replacing the placenta by an external oxygenator. In *in vivo* experiments with lambs, haemodynamic changes were observed in the umbilical artery (UA) post-connection to the AP: decrease in flow pulsatility index (PI), increase in mean pressure and heart rate, and flatter diastolic flow with a secondary peak.

Computational models can help to understand the causes of observed phenomena. Therefore, the clinical objective of this work was to investigate the causes of the aforementioned changes in UA velocity, while the methodological objective was to implement a computational model capable of reproducing the behaviour of an AP.

We used a closed lumped model of the whole fetal circulation, modified to include the AP, and tested the haemodynamic changes in the UA after altering heart rate and AP's resistance and compliance. We also added a simple wave reflection model and studied its effect on pressure and flow traces. We found that reducing AP's resistance increased mean flow, and reducing compliance decreased velocity PI. When adding the reflection model, we were able to reproduce the flatter diastolic flow observed in the UA.

This study suggests that the observed haemodynamics changes in the UA post-connection to the AP are due to a combination of decreased compliance and resistance, as well as wave reflections from components within the AP circuit.

Keywords: Artificial placenta · Fetal cardiology · Lumped cardiovascular model · Ultrasound · Wave reflection.

1 Introduction

Preterm birth is a leading cause of neonatal death [1]. Individuals born extremely premature, before 28 weeks of gestation (GA) according to the World Health Organisation (WHO) [1], account for the majority of these deaths, given that they get oxygen and nutrients through the placenta, since their organs are still underdeveloped. Consequently, these individuals are not prepared for ex-uterine life [6, 12].

Therefore, a promising approach to improve their survival is to connect them to an artificial placenta (AP) [8, 3, 11]. The fetus is surgically removed from the uterus and connected through the umbilical cord to a pumpless circuit, where the placenta is replaced by an external low resistance oxygenator. This allows the fetus to continue gestation in an artificial environment that provides oxygen and nutrients through the oxygenator.

In *in vivo* experiments with lambs, specific (Doppler-based) haemodynamic changes have been observed in the umbilical artery (UA) when the fetus is connected to an AP [10]. Specifically, diastolic velocity becomes constant with a small secondary peak, while pulsatility index (PI) decreases and mean flow, pressure and heart rate (HR) increase, which can be harmful and potentially lead to heart failure and ascites.

These changes may be explained by differences in the impedance between the biological and AP, the latter being less resistant and more rigid (less compliant). In addition, the natural placenta is optimised to maximise efficiency and avoid reflections [4]. It is composed of multiple ramifications and small subdivisions that act as wave-traps, in contrast to the filter-like oxygenator. Therefore, jointly with the cannula material properties being different from the natural vessels, the probability to have wave reflections (WR) is higher.

Computational models have been widely used to facilitate the study of the cardiovascular system, the mechanisms of haemodynamics and the relationships between its elements. To investigate the global distributions of blood flow and pressure under a range of physiological conditions and the interactions between the elements of the cardiovascular system, 0D models are generally used [16]. With this approach, a complete and consistent description is provided, and some fetal variables that are difficult to examine by non-invasive measurements can be investigated [14]. Previously published papers have modelled WR at the maternal-fetal interface [5, 15], but the AP has been overlooked.

The objective of this work was to use computational models to investigate the potential causes of the changes in haemodynamic patterns observed in the UA when connecting a fetus to an AP, which we hypothesised to be a combination of the difference in placental impedance and the presence of WR. Our contributions are the implementation of WR at the oxygenator of an existing 0D lumped model of the cardiovascular system, and the simulation of the changes produced by the connection to the AP.

2 Methodology

2.1 *In vivo* experiments

110 days lamb fetuses (equivalent of a 23 weeks GA human fetus' pulmonary development [11]) were delivered by caesarean section, and connected to the AP circuit consisting of an approximately 40 cm long 1/4" x 1/16" soft polyvinyl chloride (PVC) tube (Sorin Group) and a hollow fiber oxygenator (Quadrox-ID Neonatal Oxygenator, Maquet), thanks to a polyurethane (PUR) cannula. Both UA were trimmed at a distance of approximately 6-8 cm. The oxygenator output was connected to the umbilical vein via another PVC tube and PUR cannula (Fig. 1A). Pressure and velocity in the intra-abdominal section of the UA immediately before and after the connection to the circuit were acquired via an intravascular catheter (Millar Mikro-Tip) and Doppler ultrasound Vivid iQX (General Electric). These devices were not synchronised and no electrocardiogram was recorded. The experimental procedure was approved by the local Animal Experimental Ethics Committee (code 11314).

2.2 Lumped model

To study gross haemodynamic changes, we implemented a closed lumped model of the entire fetal circulation as described by Pennati *et al.* [14] in Matlab Simulink (Mathworks, vR2021b). Model parameters were scaled using the method proposed in [13] to simulate a 23 week GA fetus from the original 38 weeks model. The model consists of two distinct sections: the heart, with both ventricles and atria, which are modeled as time-varying elastances and the valves; and the blood circulation represented by 19 elements, combining arterial segments (RLC) and vascular bed compartments (RC), among which is the placenta. As shown in Fig. 1B, both biological and AP are modelled as a 2 element Windkessel, upstream connected to the UA resistor and downstream attached to the umbilical vein capacitor. The pressures and blood flows reported in this work were measured between the UA resistor and the placental capacitor.

In order to evaluate how the decrease in the placental impedance and the increase in HR influence the haemodynamics in the UA, placental resistance (R_{plac}) and compliance (C_{plac}) were decreased up to a 2-fold decrease, and HR was systematically increased from 130 to 220 beats per minute (bpm), while the remaining parameters were kept unchanged.

2.3 Wave reflections

Pressure (P) and flow (Q) in the cardiovascular system propagate as waves [2], and therefore can be decomposed in a forward and backward wave, each moving with a wave speed c:

$$Q(x,t) = Q_f(x+ct) - Q_b(x-ct); \qquad P(x,t) = P_f(x+ct) + P_b(x-ct) \quad (1)$$

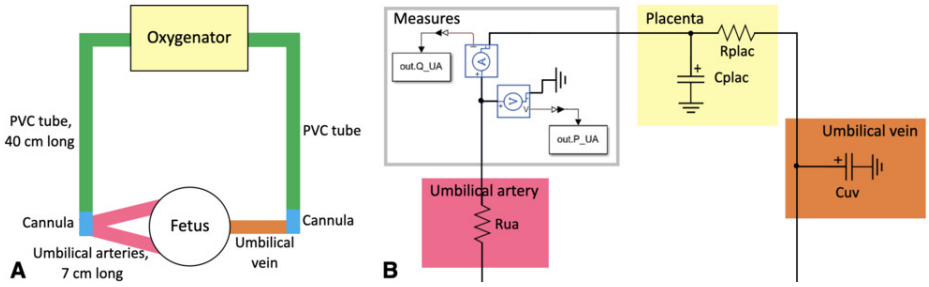

Fig. 1. (A) Scheme of the experimental setup and (B) equivalent lumped computational model of the placenta section, indicating where the UA blood flow and pressure are measured.

with x being the position and t the time. Note that pressure waves are added, while flow waves are subtracted since blood moving backwards counteracts the blood moving forwards. The wave speed c, also called pulse wave velocity (PWV), can be computed from the geometry and material characteristics of the vessel using Korteweg-Moens equation [7]:

$$c = \sqrt{\frac{Eh}{2r\rho}} \tag{2}$$

where E is the Young modulus, h the wall thickness, r the vessel radius and ρ the blood density. When flow/pressure forward waves encounter a change in PWV, for instance due to a change in the vessel properties, a backward wave is generated, with an intensity depending on the reflection coefficient Γ:

$$Q_b = \Gamma Q_f; \qquad P_b = \Gamma P_f \tag{3}$$

The reflection coefficient Γ depends on the difference of the PWV between the two media (a and b):

$$\Gamma = \frac{c_a - c_b}{c_a + c_b} \tag{4}$$

To assess the effect of WR in the UA, we added a simple reflection model to our lumped model, in which the UA flow (Q_{UA}) and pressure (P_{UA}) were considered to be a combination of original (Q_f,P_f), travelling forward, and reflected waves (Q_b,P_b), travelling backwards, satisfying the relationship of Eq. 3. The time delay (Δt), the phase shift between the forward and backward waves, was calculated from the PWV and the distance to the reflection origin.

Two possible WR origins were considered, the UA-PVC tube and the PVC tube-oxygenator interfaces. For the first case, Γ and Δt were estimated by assuming 7 cm of UA and computing the PWV in each material. For the second case, Δt was computed by assuming 7 cm of UA and 40 cm of PVC tube. However, the PWV in the oxygenator could not be calculated due to its complex geometry, so Γ could not be estimated. Therefore, the previous Γ was used and then we did

Table 1. Quantitative measurements of the velocity (v) and pressure (P) traces pre- (first value) and post-connection to the AP (second value).

Indicator	**Subject**				**Average**
	#1	#2	#3	#4	
Heart rate (bpm)	131/205	134/210	141/245	124/147	133/202
FWHM P/v ratio	0.9/1.4	0.8/1.3	0.8/1.2	0.8/1.0	0.9/1.2
Pulsatility index	1.5/0.7	2.3/0.3	1.4/0.5	2.1/0.6	1.8/0.5
Mean pressure (mmHg)	65.4/91.7	38.7/37.2	32.5/97.9	49.6/61.5	46.5/72.1
Mean velocity (cm/s)	38.7/42.3	22.4/41.0	33.2/72.9	31.4/43.1	31.4/49.8

a parametric analysis changing its value to study the effect of different reflection coefficients. The parameters needed to compute the PWV in the UA were extracted from the literature [9, 17], and those of the PVC from the manufacturer's specifications, except for the Young modulus which was measured.

2.4 Signal analysis of pressure and flow traces

Several haemodynamic parameters were calculated to quantify both real and simulated blood flow velocity and pressure waveforms including: their mean value pre- and post-connection to the AP, the pressure/flow full width at half maximum (FWHM) ratio, and the velocity PI. FWHM was defined as the difference between the two instants of time when the curve is equal to half its maximum value [18]. Also, PI was defined as the difference between the maximum systolic velocity and the minimum diastolic velocity divided by the mean velocity.

3 Results

3.1 *In vivo* pressure and flow signal analysis

The collected Doppler velocity and catheter pressure traces of 4 individuals, measured at the UA, pre- and post-connection to the AP, are displayed in Fig. 2. Note that data acquired were not time-synchronised due to experimental limitations, thus ventricular systole and diastole could not be indicated on the plots. We can observe two main changes in the velocity profile: a decrease in PI and a profile change in diastole, that before intervention presented an exponential decay, and after intervention is transformed into a rapid decay followed by an almost constant phase. In the pressure traces we can observe an increase in mean pressure.

Table 1 shows the quantitative haemodynamic indicators for all 4 subjects and the population average, before and after intervention. They show an increase in heart rate, mean pressure and velocity and FWHM pressure/velocity ratio, and a decrease in the UA PI after intervention.

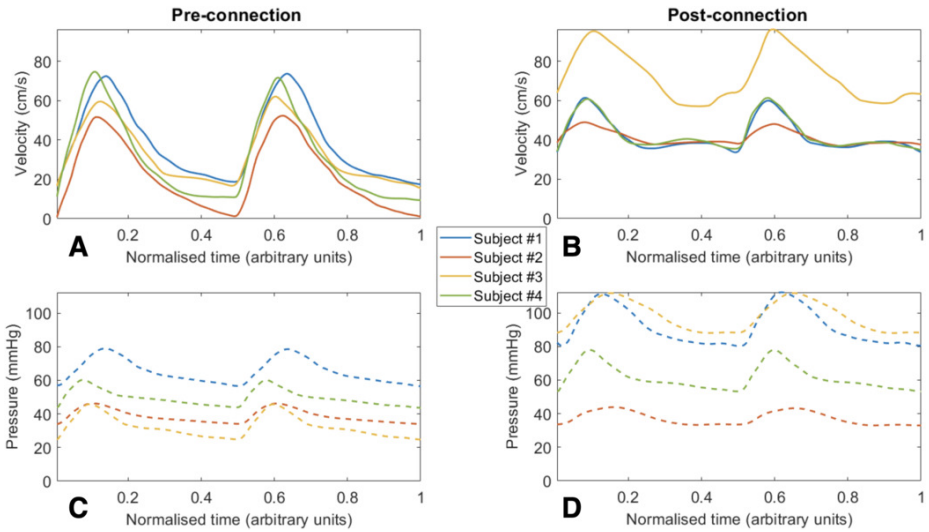

Fig. 2. UA Doppler velocity traces (A) pre- and (B) post-connection to the AP, and their corresponding (C) pre- and (D) post-connection to the AP pressure traces of 4 individuals. Ventricular systole and diastole could not be depicted due to the lack of synchronisation.

3.2 Lumped model of the artificial placenta

We simulated the after-intervention haemodynamics in a lumped model of a 23 GA fetus by lowering the compliance and resistance of the placental component, as the oxygenator is stiffer and less resistant than the natural placenta, as well as increasing the HR. Results are displayed in Fig. 3, where each change is analysed separately. Ventricular systole and diastole are indicated on the graphs, although they may not be as accurate as in the heart. Lowering compliance decreased flow PI and increased pressure PI, lower resistances increased blood flow and decreased pressures, and higher heart rates resulted in lower PI. Afterwards, we manually selected the combination of HR = 200 bpm, $C_{plac} = 0.0033$ ml/mmHg and $R_{plac} = 1.796$ mmHg·s/ml as with these values we obtained the shape of the traces most similar to the real ones, although mean pressure and PI were still not very realistic. The simulated curves obtained with these values are displayed in Fig. 3D.

3.3 Wave reflections

We used the simple WR model to simulate possible WR at the UA-PVC interface or at the oxygenator level. Using the equations described in Section 2.3, we computed the theoretical PWV for the UA and PVC, obtaining 6.44 m/s and 39.02 m/s, respectively. For WR originated at the UA-PVC interface, Γ was estimated to be 0.72 and the time delay Δt to be 0.022 s, assuming 7 cm of UA.

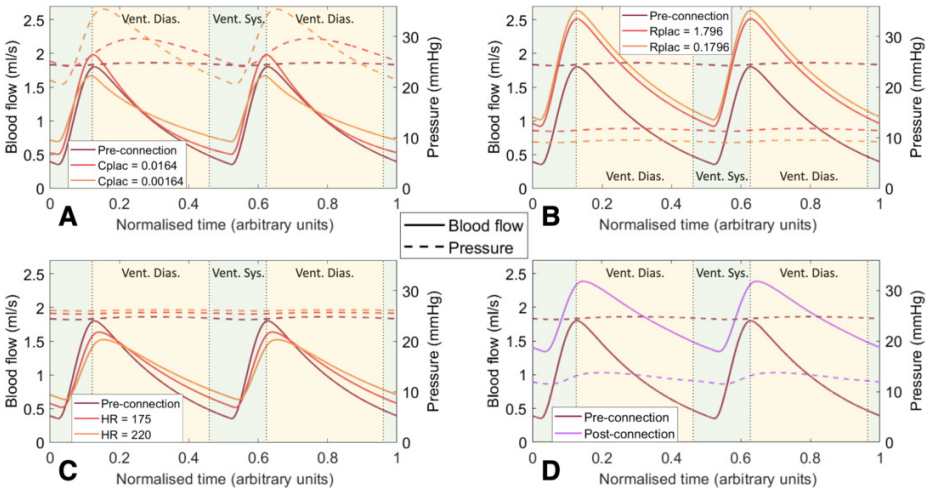

Fig. 3. Simulated UA blood flow (solid line) and pressure (dashed line) for a subject connected to the AP, with different values of (A) placental compliance, (B) placental resistance and (C) heart rate of the subject. In (D) the pre-connection and post-connection (HR = 200 bpm, $C_{plac} = 0.0033$ ml/mmHg and $R_{plac} = 1.796$ mmHg·s/ml) results are compared. Ventricular systole and diastole are depicted in green and yellow, respectively.

For WR originated at the PVC-oxygenator interface, the previous value of Γ was considered, and Δt was computed to be 0.042 s, assuming 7 cm of UA and 40 cm of PVC.

We added WR to the pressure and velocity traces obtained from the lumped model with AP to qualitatively compare the patterns. The resulting curves are shown in Fig. 4A and the quantitative measurements in Table 2. When WR model was added, we observed that UA pressure increased while UA flow decreased. We also observed that the diastolic UA flow had two differentiated phases as measured experimentally: a first phase of fast deceleration and a second phase of constant velocity, while without considering WR, diastolic flow decreased exponentially. Reflections generated at the oxygenator presented more pulsatility and a more flattened second phase of the flow with respect to WR at the UA-PVC interface.

We did a parametric analysis of Γ at the oxygenator level from 0.55 to 0.85 (Fig. 4B), maintaining Δt at 0.042 s. For higher Γ the pressure increased and the blood flow decreased, and the velocity decelerated faster.

4 Discussion

We implemented a 0D model of the fetal circulation at 23 weeks GA to study the haemodynamic changes in the UA produced by the connection of the fetus to an AP. While the pre-connection model flows were realistic, pressure traces

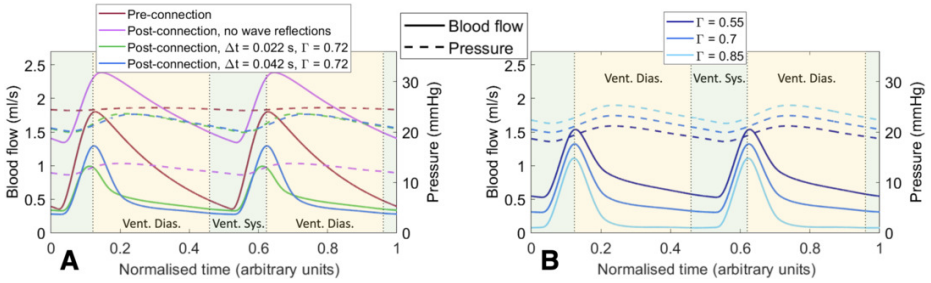

Fig. 4. Simulated UA blood flow (solid line) and pressure (dashed line) (A) pre-connection and post-connection to the AP, both with and without the WR model, and (B) considering WR with different values of reflection coefficient (Γ) at the oxygenator level. Ventricular systole and diastole are depicted in green and yellow, respectively.

Table 2. Quantitative measurements of the velocity (v) and pressure (P) traces pre- and post-connection to the AP for the experimental data average and simulations with and without considering WR at different interfaces.

Indicator	**Exp. data**	**No WR**	**UA-PVC**	**PVC-oxygenator**
Heart rate (bpm)	133/202	130/200	130/200	130/200
FWHM P/v ratio	0.9/1.2	1.5/1.2	1.5/2.9	1.5/2.7
Pulsatility index	1.8/0.5	1.5/0.6	1.5/1.3	1.5/2.1
Mean pressure (mmHg)	46.5/72.1	24.6/12.8	24.6/22.0	24.6/22.0
Mean velocity (cm/s)	31.4/49.8	25.1/47.4	25.1/13.1	25.1/13.1

presented low PI compared to the real ones. Lowering compliance and resistance to model the AP resulted in an increase in UA blood flow and reduced PI, matching real-data, but also a pressure drop that contradicted experimental observations. This was expected, as according to Ohm's law a lower resistance increases blood flow and reduces blood pressure. Moreover, simulated diastolic velocities presented an exponential decay rather than experimental data's flat profile. This could be explained by the presence of secondary waves that modulate the velocity.

We introduced a model of WR and assessed their impact on the blood flow and pressure patterns. By including the WR model, we were able to mimic the increase in FWHM pressure/velocity ratio, as part of the forward wave was counterbalanced by the backwards, thus increasing the width of the flow curve and flattening the velocity in diastole, two important patterns that were observed in experimental data. Also, higher Γ decreased the mean flow and increased the mean pressure, as was expected from Eq. 1. However, WR produced a mean pressure similar to pre-connection values, but with a significantly lower mean flow, which consequently increased the PI, despite the fact that the absolute pulsatility was lower. We hypothesise that in a real heart, there would be a pressure increase to elevate the blood flow, which would result in a preserved flow and much higher pressure, but these adaptation mechanisms are not present in

our simplified model. Moreover, there could be multiple WR that would increase the blood flow and that a 0D model is not able to capture, but a 1D model could.

Limitations While we could reproduce experimental data waveforms, our model had limitations. First, we used a non-personalised human model, while lambs were used in the real experiments, thus the match between the real and simulated traces was not to be expected. Secondly, we only modelled changes in the placental segment, and did not consider cardiac remodelling triggered by the removal from the natural environment, that would likely lead to increased blood flow. Thirdly, the WR model is purely phenomenological, and did not consider multiple reflections, for which a 1D model should be used. Finally, only data from 4 real subjects were provided, so no meaningful statistical test could be performed.

5 Conclusions

This study suggests that the observed changes in UA blood flow and pressure patterns, when connecting a fetus to an AP, are due to a combination of decreased placenta's compliance and resistance, as compared to a biological placenta, as well as the occurrence of WR from components within the AP circuit. In a future work, a 1D personalised model should be implemented in order to model the probable multiple WR present in the experiments.

6 Acknowledgements

The research leading to these results has received funding from "la Caixa" Banking Foundation. This work has been performed under FI 2022 grant number 00237, awarded by the Agency for Management of University and Research Grants (AGAUR), Generalitat de Catalunya.

References

1. Newborn Mortality, https://www.who.int/news-room/fact-sheets/detail/levels-and-trends-in-child-mortality-report-2021#: :text=Preterm birth%2C intrapartum-related complications,causes of most neonatal deaths
2. Bramwell, J.C., Hill, A.V.: The velocity of pulse wave in man. Proceedings of the Royal Society of London. Series B, Containing Papers of a Biological Character **93**(652), 298–306 (apr 1922). https://doi.org/10.1098/rspb.1922.0022, https://royalsocietypublishing.org/doi/10.1098/rspb.1922.0022
3. Bryner, B., Gray, B., Perkins, E., Davis, R., Hoffman, H., Barks, J., Owens, G., Bocks, M., Rojas-Peña, A., Hirschl, R., Bartlett, R., Mychaliska, G.: An extracorporeal artificial placenta supports extremely premature lambs for 1 week. Journal of Pediatric Surgery **50**(1), 44–49 (2015). https://doi.org/10.1016/j.jpedsurg.2014.10.028
4. Cahill, L.S., Stortz, G., Ravi Chandran, A., Milligan, N., Shinar, S., Whitehead, C.L., Hobson, S.R., Ayyathurai, V., Rahman, A., Saghian, R., Jobst, K.J., McShane, C., Block-Abraham, D., Seravalli, V., Laurie, M., Millard, S., Delp, C., Wolfson, D., Baschat, A.A., Murphy, K.E., Serghides, L., Morgen, E., Macgowan, C.K., Parks, W.T., Kingdom, J.C., Sled, J.G.: Wave reflections in the umbilical artery measured by Doppler ultrasound as a novel predictor of placental pathology. EBioMedicine **67**, 103326 (2021). https://doi.org/10.1016/j.ebiom.2021.103326, https://doi.org/10.1016/j.ebiom.2021.103326
5. Hill, A.A., Surat, D.R., Cobbold, R.S.C., Langille, B.L., Mo, L.Y.L., Adamson, S.L.: A wave transmission model of the umbilicoplacental circulation based on hemodynamic measurements in sheep. American Physiological Society (1995)
6. Howson, C.P., Kinney, M., McGougall, L., Lawn, J.: Born too soon : the global action report on preterm birth. Reproductive Health p. 9 (2013). https://doi.org/10.1186/1742-4755-10-S1-S1
7. Korteweg, D.J.: Ueber die Fortpflanzungsgeschwindigkeit des Schalles in elastischen Röhren. Annalen der Physik pp. 525–542 (1878). https://doi.org/10.1002/andp.18782411206
8. Miura, Y., Matsuda, T., Funakubo, A., Watanabe, S., Kitanishi, R., Saito, M., Hanita, T.: Novel modification of an artificial placenta: Pumpless arteriovenous extracorporeal life support in a premature lamb model. Pediatric Research **72**(5), 490–494 (nov 2012). https://doi.org/10.1038/pr.2012.108
9. Myers, L.J., Capper, W.L.: A transmission line model of the human foetal circulatory system. Medical Engineering and Physics **24**(4), 285–294 (2002). https://doi.org/10.1016/S1350-4533(02)00019-X
10. Ozawa, K., Davey, M.G., Tian, Z., Hornick, M.A., Mejaddam, A.Y., McGovern, P.E., Flake, A.W., Rychik, J.: Fetal echocardiographic assessment of cardiovascular impact of prolonged support on EXTrauterine Environment for Neonatal Development (EXTEND) system. Ultrasound in Obstetrics and Gynecology **55**(4), 516–522 (apr 2020). https://doi.org/10.1002/uog.20295
11. Partridge, E.A., Davey, M.G., Hornick, M.A., McGovern, P.E., Mejaddam, A.Y., Vrecenak, J.D., Mesas-Burgos, C., Olive, A., Caskey, R.C., Weiland, T.R., Han, J., Schupper, A.J., Connelly, J.T., Dysart, K.C., Rychik, J., Hedrick, H.L., Peranteau, W.H., Flake, A.W.: An extra-uterine system to physiologically support the extreme premature lamb. Nature Communications **8** (2017). https://doi.org/10.1038/ncomms15112

12. Patel, R.M., Kandefer, S., Walsh, M.C., Bell, E.F., Carlo, W.A., Laptook, A.R., Sánchez, P.J., Shankaran, S., Van Meurs, K.P., Ball, M.B., Hale, E.C., Newman, N.S., Das, A., Higgins, R.D., Stoll, B.J.: Causes and Timing of Death in Extremely Premature Infants from 2000 through 2011. New England Journal of Medicine **372**(4), 331–340 (jan 2015). https://doi.org/10.1056/nejmoa1403489
13. Pennati, G., Fumero, R.: Scaling approach to study the changes through the gestation of human fetal cardiac and circulatory behaviors. Annals of biomedical engineering **28**(4), 442–452 (2000). https://doi.org/10.1114/1.282
14. Pennati, G., Bellotti, M., Fumero, R.: Mathematical modelling of the human foetal cardiovascular system based on Doppler ultrasound data. Medical Engineering and Physics **19**(4), 327–335 (1997). https://doi.org/10.1016/S1350-4533(97)84634-6
15. Saghian, R., Cahill, L., Rahman, A., Steinman, J., Stortz, G., Kingdom, J., Macgowan, C., Sled, J.: Interpretation of wave reflections in the umbilical arterial segment of the feto-placental circulation: Computational modeling of the feto-placental arterial tree. IEEE Transactions on Biomedical Engineering **68**, 3647–3658 (12 2021). https://doi.org/10.1109/TBME.2021.3082064
16. Shi, Y., Lawford, P., Hose, R.: Review of zero-d and 1-d models of blood flow in the cardiovascular system. BioMedical Engineering Online **10** (4 2011). https://doi.org/10.1186/1475-925X-10-33
17. Van Den Wijngaard, J.P., Westerhof, B.E., Faber, D.J., Ramsay, M.M., Westerhof, N., Van Gemert, M.J.: Abnormal arterial flows by a distributed model of the fetal circulation. American Journal of Physiology - Regulatory Integrative and Comparative Physiology **291**(5), 1222–1233 (2006). https://doi.org/10.1152/ajpregu.00212.2006
18. Weisstein, E.W.: Full Width at Half Maximum – from Wolfram MathWorld, https://mathworld.wolfram.com/FullWidthatHalfMaximum.html